Amino Acids (2015) 47:2385–2397
DOI 10.1007/s00726-015-2029-7

ORIGINAL ARTICLE

Antimicrobial activity and membrane-active mechanism of tryptophan zipper-like β-hairpin antimicrobial peptides

Lin Xu[1,2] · Shuli Chou[1] · Jiajun Wang[1] · Changxuan Shao[1] · Weizhong Li[1] · Xin Zhu[1] · Anshan Shan[1]

Received: 22 January 2015 / Accepted: 10 June 2015 / Published online: 19 June 2015

Abstract Antimicrobial peptides (AMPs) with amphipathic β-hairpin structures have been demonstrated to possess potent antimicrobial activities and great cell selectivities. However, our understanding of β-hairpin antimicrobial peptides lags behind that of α-helices, mainly because it is difficult for short peptides to form robust β-hairpin structures. Tryptophan zipper (trpzip) peptides are among the most stable β-hairpin peptides known to fold spontaneously without requiring covalent disulfide constraint or metal binding. To develop model β-hairpin AMPs with small size and remarkable stability, a series of amphiphilic linear peptides were designed based on the trpzip motif. The sequence of designed peptides is $(WK)_n^DPG(KW)_n$-NH_2 (n = 1, 2, 3, 4, 5), and the antimicrobial activity and membrane interaction mechanism of the peptides were evaluated. The results showed that these peptides readily fold into β-hairpin structures in aqueous and membrane-mimicking environments and exhibit broad-spectrum antimicrobial activities against both gram-positive and gram-negative bacteria. The antibacterial potency of the peptides initially increased and then decreased with increasing chain length. WK3, a 14-residue peptide, displayed excellent antimicrobial activity with minimal hemolytic activity and cytotoxicity, suggesting that it possesses great cell selectivity. Scanning electron microscopy (SEM), transmission electron microscopy (TEM), fluorescence spectroscopy, and flow cytometry indicated that representative peptides WK3 and WK4 exert their activities by permeabilizing the microbial membrane and damaging cell membrane integrity. This study reveals the application potential of the designed peptides as promising antimicrobial agents for the control of infectious diseases, and it also provides new insights into the design and optimization of highly stable β-hairpin AMPs with great antimicrobial activities and cell selectivities.

Keywords Antimicrobial peptides · Tryptophan zipper · β-Hairpin · Cell selectivity · Bactericidal mechanism

Abbreviations

AMP	Antimicrobial peptide
Trpzip	Tryptophan zipper
MIC	Minimum inhibitory concentration
MHC	Minimal hemolytic concentration
hRBCs	Human red blood cells
TI	Therapeutic index
CD	Circular dichroism
SDS	Sodium dodecyl sulfate
PI	Propidium iodide
MH	Mueller–Hinton

Introduction

The extensive and sometimes indiscriminate use of antibiotics in clinical practice has led to the rising prevalence of medically relevant multidrug-resistant pathogens, making infectious diseases increasingly difficult to control with conventional antibiotics. Therefore, the development of new classes of antimicrobial agents with high potency and

Handling Editor: F. Albericio.

✉ Anshan Shan
asshan@neau.edu.cn

[1] Institute of Animal Nutrition, Northeast Agricultural University, 59 Mucai Street, Harbin 150030, China

[2] Heilongjiang Polytechnic, 5 Xuefu Road, Harbin 150080, China

a distinct mode of action that disfavors drug resistance is a challenging endeavor. Antimicrobial peptides (AMPs) are evolutionarily conserved components of the innate immunity systems of organisms. They have a broad spectrum of activities against various bacteria, fungi, viruses, parasites, and even cancer cells (Baek and Lee 2010; Chen et al. 2014; Takiguchi et al. 2014; Torrent et al. 2012). Furthermore, unlike conventional antibiotics which have specific intracellular targets that can be easily mutated by bacteria to gain resistance, the majority of AMPs exert their activities via the physical disruption of microbial membrane integrity to cause leakage of cytoplasmic components, leading to cell death (Ong et al. 2013; Teixeira et al. 2012). The physically destructive nature of microbial cell membranes is believed to prevent the development of microbial resistance toward AMPs because this would require microorganisms to alter their entire membrane lipid compositions (Gopal et al. 2013). Due to these inherent advantages, the investigation and exploitation of AMPs have been regarded as a potential source of new therapeutic strategies for protection against multidrug-resistant bacteria.

Despite the clear potential of AMPs, obstacles such as costliness, systemic toxicities, in vivo stability, and a lack of information about structure–activity relationships may ultimately compromise the therapeutic applications of these peptides as antimicrobial agents (Brogden and Brogden 2011). In addition, some reports suggest that the direct clinical use of endogenous peptides or analogs with sequences that are too close to the host defense AMPs might potentially promote resistance to innate AMPs, compromising the natural defenses of the host and causing security threats to public health and the environment (Bell and Gouyon 2003). Therefore, the design of short AMPs bearing minimal homology to naturally occurring sequences is considered to be a viable approach for the development of safe and effective antibacterial agents for clinical application (Ong et al. 2013).

The most important regular secondary structures found in antimicrobial peptides are the α-helices and β-sheets. There is growing evidence to indicate that naturally occurring AMPs with amphipathic β-sheet structures possess potent antimicrobial properties typified by protegrin-1 (PG-1) and tachyplesin-1 (TP-1) (Fjell et al. 2011). More importantly, compared to their α-helical counterparts of equal hydrophobicity and charge, synthetic β-sheet peptides have been shown to have greater selectivities for bacterial cells while retaining similar antimicrobial activities (Jin et al. 2005). Considerable efforts have been devoted to the design and optimization of α-helical peptide sequences that possess enhanced antimicrobial activities coupled with low toxicities to host cells; however, systematic studies on β-sheet-forming peptides are acutely lacking in comparison, largely because it is difficult for short peptides to form robust β-structures (Dong et al. 2006; Ong et al. 2013). In particular, most existing β-sheet AMPs require one or more internal disulfide bridges as conformational constraints to stabilize their bioactive conformations, which dramatically increases the cost for large-scale manufacturing of the peptides (Dong et al. 2012). Furthermore, disulfide bridges have disadvantages as structural stabilizers of bioactive peptides because they can be cleaved in vivo by reaction with free thiol groups, leading to the inevitable loss of fold stability and biological activity (Obrecht et al. 2012). Therefore, the development of highly stable, linear β-sheet model systems has been an important step forward and promoted structure–function studies of β-sheet peptides.

As a basic and simplified model of β-sheet structure, a β-hairpin consists of a single sequence folded back on itself to generate two antiparallel strands connected by a turn. Some of the most stable β-hairpin peptides designed to date are tryptophan zipper (trpzip) peptides, which are linear peptides containing one or two Trp–Trp cross-strand pairs at non-hydrogen-bonded sites (Cochran et al. 2001; Eidenschink et al. 2009; Santiveri et al. 2011; Takekiyo et al. 2009; Wu et al. 2012). These peptides are among the shortest β-hairpin peptides known to fold spontaneously without requiring disulfide crosslinks or metal binding. Remarkably, for small β-hairpins, trpzips have much higher stabilities than other β-hairpin peptides of similar size, and their thermodynamic properties are comparable to those of protein domains (Santiveri and Jiménez 2010). The extreme stability of trpzip peptides arises from cross-strand Trp–Trp interactions, which have been shown to be a better structure stabilizer than other hydrophobic interactions and even covalent disulfide bonds (Mirassou et al. 2009; Santiveri et al. 2008). The small size and remarkable stability of trpzip peptides make them very attractive as templates for the design of bioactive molecules. To date, some studies have described the development of functional peptides based on the trpzip scaffold, including nucleotide receptors, rubredoxin mimics, peptide ligands, and inhibitors of amyloid formation (Butterfield and Waters 2003; Hopping et al. 2013; Kim et al. 2012; Nanda et al. 2005). However, the biological activities of designed β-hairpin antimicrobial peptides with trpzip motifs have not been studied.

In the present study, we adopted a facile approach to design a series of linear trpzip-like β-hairpin AMPs by drawing upon the advantageous features of natural AMPs and trpzip peptides, including (a) the pairwise tryptophan residues at non-hydrogen-bonded sites that stabilize the β-hairpin conformation through cross-strand interactions (Santiveri et al. 2011), (b) the requirement for cationic residues to mediate peptide interactions with negatively charged bacterial membranes, and (c) the amphipathic arrangement of cationic and hydrophobic residues (Takahashi et al. 2010). The effect of the peptide chain length

on antimicrobial activity was evaluated against gram-negative bacteria (*Escherichia coli* and *Salmonella pullorum*), gram-positive bacteria (*Staphylococcus aureus* and *S. epidermidis*), and methicillin-resistant bacteria (*S. aureus* ATCC 43300). The hemolytic and cytotoxic activities of peptides were further determined in comparison with natural β-hairpin AMP PG-1, and the peptide with the greatest cell selectivity was identified. In addition, scanning electron microscopy (SEM), transmission electron microscopy (TEM), outer membrane (OM) permeabilization, cytoplasmic membrane depolarization, and flow cytometric assays were employed to investigate the peptide-membrane interaction mechanisms of the peptides. The overall objective of this study is to provide an effective strategy for the design or optimization of linear β-hairpin AMPs with excellent antimicrobial activities and cell selectivities.

Materials and methods

Peptide synthesis

The peptides used in this study were synthesized using the solid-phase method with Fmoc chemistry by GL Biochem (Shanghai, China), and their purities were confirmed to be >95 % using analytical reverse-phase high-performance liquid chromatography (HPLC). Matrix-assisted laser desorption/ionization time-of-flight mass spectroscopy (MALDI-TOF MS, Linear Scientific Inc., USA) was used to further determine the molecular masses of the peptides. The peptides were then dissolved in deionized water at a concentration of 2.56 mM and stored at −20 °C for subsequent assessments.

CD analysis

Circular dichroism (CD) experiments were performed to determine the secondary structures of the peptides in different environments. CD spectra were obtained at a peptide concentration of 150 μM in 10 mM sodium phosphate buffer (pH 7.4) and 30 mM SDS micelles (Sigma). The peptide samples were measured at room temperature (25 °C) with a J-820 spectropo-larimeter (Jasco, Tokyo, Japan) equipped with a rectangular quartz cell with a path length of 1 mm. The CD spectra were recorded at a scanning speed of 10 nm/min over the wavelength range of 190–250 nm. An average of over three scans was collected for each peptide. The mean residue ellipticity was calculated from the equation: $\theta_M = (\theta_{obs} \times 1000)/(l \times c \times n)$, where θ_M is mean residue ellipticity (°cm^2/dmol), θ_{obs} is the observed ellipticity corrected for the buffer at a given wavelength (m°), l is the path length (mm), c is peptide concentration (mM), and n is the number of residues. The secondary content of the peptides was calculated online using K2D2 (http://k2d2.ogic.ca/).

Antimicrobial assays

The antimicrobial activities of the peptides were investigated against the following bacterial strains: *S. aureus* ATCC 29213, *S. aureus* ATCC 43300 (methicillin-resistant strain), *S. epidermidis* ATCC 12228, *E.* ATCC 25922, *E. coli* UB1005, and *Salmonella Pullorum* C7913. The minimal inhibitory concentrations (MICs) of the peptides were determined using a modified standard microtiter dilution method, as described previously (Ma et al. 2012). Briefly, bacterial cells were cultivated in Mueller–Hinton broth (MHB, Sigma) at 37 °C under shaking at 300 rpm to reach mid-logarithmic phase and then diluted to 0.5–1 × 10^6 CFU/ml. Subsequently, 50 μl portions of the microorganism suspensions were incubated in 96-well microtiter plates with 50 μl of two-fold serially diluted peptides at different concentrations (0.25–128 μM). The MICs were defined as the lowest peptide concentrations that completely inhibited bacterial growth after 16 h of incubation at 37 °C. Cultures without peptides and uninoculated MHB were employed as positive and negative controls, respectively. Each test was reproduced at least four times using three replicates.

Measurement of hemolytic activity

Fresh human red blood cells (hRBCs) were obtained by centrifuging whole blood at 1000×*g* for 5 min at 4 °C. The erythrocytes were washed three times with phosphate-buffered saline (PBS, pH 7.2) and then resuspended in PBS to attain a dilution of approximately 1 % (v/v) of the erythrocyte. The erythrocyte solution (50 μl) was incubated with 50 μl of serially diluted peptides (0.5–256 μM) dissolved in PBS for 1 h at 37 °C. After centrifugation (1000×*g*, 5 min, 4 °C), the supernatant was transferred to a 96-well plate. The hemolysis was monitored by measuring the optical density (OD) at 570 nm. The hRBCs in PBS without peptides and 0.1 % (v/v) Triton X-100 were used as negative and positive controls, respectively. Each measurement was conducted in triplicate. Minimal hemolytic concentrations (MHCs) were defined as the peptide concentrations causing 5 % hemolysis.

Cytotoxicity assay

The colorimetric 3-(4,5-dimethylthiazol-2-yl)-2,5-diphenyltetrazolium bromide (MTT) dye (Sigma) reduction assay was performed to determine the cytotoxicity of each peptide on the murine macrophage cell line RAW264.7, as described previously (Dong et al. 2014). Briefly, the cells were pre-seeded on a 96-well plate at a density of 2 × 10^5

cells/ml in Dulbecco-modified Eagle medium (DMEM) and then incubated overnight under a fully humidified atmosphere of 95 % air and 5 % CO_2 at 37 °C. The next day, cell cultures were treated with 50 μl of two-fold diluted peptide solutions (0.25–128 μM) and incubated for 24 h at 37 °C. Wells containing untreated cells served as controls. MTT (50 μl, 0.5 mg/ml) was added into each well, and the plate was incubated for a further 5 h at 37 °C. The cells were then centrifuged at 1000×*g* for 5 min, and the supernatants were discarded. Subsequently, 150 μl of dimethyl sulfoxide (DMSO) was added to dissolve the precipitated formazan crystals, and the OD at 492 nm was recorded using a microplate reader (Tecan GENios F129004, Austria).

Scanning electron microscopy (SEM) characterization

Bacterial cells *S. aureus* ATCC29213 and *E. coli* ATCC25922 were cultured in MHB at 37 °C to an exponential phase, harvested by centrifugation at 1000×*g* for 10 min, washed twice with 10 mM PBS, and resuspended to an OD600 of 0.2. The cell suspensions were incubated for 30 min at 37 °C with different peptides at their 1 × MICs. Controls were run without peptides. After incubation, the cells were harvested by centrifugation and washed thrice at 5000×*g* for 5 min at 4 °C with PBS. Subsequently, the bacterial cells were fixated overnight with 2.5 % (v/v) glutaraldehyde at 4 °C. The fixed samples were washed twice with PBS followed by dehydration in graded ethanol solutions (50, 70, 90, and 100 %) for 15 min each. They were then transferred to a mixture (1:1, v/v) of absolute ethanol and tertiary butanol for 20 min followed by pure tertiary butanol for 30 min. After lyophilization and gold coating, the bacterial specimens were observed by SEM (Hitachi S-4800, Japan).

Transmission electron microscopy (TEM) characterization

The bacterial samples were prepared in the same way as for SEM treatment. After overnight pre-fixation with 2.5 % glutaraldehyde, the bacterial cells were washed twice and then post-fixed with 1 % osmium tetroxide for 2 h. The fixed samples were subsequently washed twice with PBS and dehydrated for 15 min in each of a graded ethanol series (50, 70, 90, and 100 %) along with for 10 min in both a mixture (1:1, v/v) of absolute ethanol and acetone and absolute acetone. Subsequently, the samples were transferred to a mixture (1:1, v/v) of absolute acetone and epoxy resin for 30 min followed by pure epoxy resin for overnight at a constant temperature. Finally, the specimens were sectioned using an ultramicrotome, double stained by uranyl acetate and lead citrate, and observed by TEM (Hitachi H-7650, Japan).

Outer membrane permeabilization assay

The outer membrane permeabilization activities of the peptides were measured using the fluorescent dye *N*-phenyl-1-naphthylamine (NPN) uptake assay, as described previously (Zhu et al. 2014). Briefly, *E. coli* UB1005 was cultivated to mid-logarithmic phase, washed twice with washing buffer (5 mM HEPES, 5 mM glucose, pH 7.4), and diluted to 0.5–1 × 10^6 CFU/ml in the same buffer. The bacterial suspension was incubated with 10 μM NPN for 15 min at 37 °C. The fluorescence intensity change was measured using an F-4500 fluorescence spectrophotometer (Hitachi, Japan) with an excitation wavelength of 350 nm and an emission wavelength of 420 nm, and the background fluorescence was recorded. The peptides were added to 2 ml of the cell suspension in a 1 cm cuvette to achieve the desired concentrations, and fluorescence was recorded until no further increase in fluorescence was observed. As the permeability of the outer membrane increased due to the addition of peptide, NPN incorporated into the outer membrane led to an increase in fluorescence. Polymyxin B (Sigma) was used as a positive control because of its strong outer membrane permeabilizing properties. The acquired fluorescence was then converted to % NPN uptake according to the equation: $\%\ \text{NPN uptake} = (F_{\text{obs}} - F_0)/(F_{100} - F_0) \times 100$, where F_{obs} is the observed fluorescence at a given peptide concentration, F_0 is the initial fluorescence of NPN with *E. coli* cells only, and F_{100} is the fluorescence of NPN upon addition of 10 μg/ml polymyxin B.

Cytoplasmic membrane depolarization assay

The abilities of the peptides to depolarize the bacterial cytoplasmic membrane were determined using the membrane potential-sensitive fluorescent dye $diSC_3$-5, as described previously (Ma et al. 2013). Briefly, mid-log phase *E. coli* UB1005 was washed twice in buffer (5 mM HEPES, 20 mM glucose, pH 7.4) and then resuspended to an OD600 of 0.05 in the same buffer. The bacterial suspension was incubated with 0.4 μM diSC3-5 for 1 h at 37 °C. Subsequently, KCl was added to equilibrate the cytoplasmic and external K^+ to a final concentration of 0.1 M. Two milliliters of the cell suspension was placed in a 1 cm cuvette, and the peptides at desired concentrations were added. The fluorescence intensity change was recorded using an F-4500 fluorescence spectrophotometer (Hitachi, Japan) with excitation and emission wavelengths of 622 and 670 nm, respectively.

Flow cytometry

The bacterial cell membrane integrity was evaluated by flow cytometry analysis (Dong et al. 2014). In brief, *E.*

coli ATCC 25922 was cultured in MHB to mid-log phase, harvested, washed thrice with PBS, and then diluted to 10^5 CFU/ml. The bacterial suspensions were incubated with the peptides (0.5 × MIC and 1 × MIC) for 30 min at 28 °C. The cells were harvested by centrifugation, washed, and then incubated with 10 μg/ml propidium iodide (PI, Sigma) for 30 min at 4 °C. After incubation, the unbound dye was removed by washing with excess PBS. A FACScan instrument (Becton–Dickinson, San Jose, CA) was used to record the data with an excitation wavelength of 488 nm. Cells incubated with PI in the absence of peptides were employed as the negative control.

Results

Peptide design and characterization

In this study, we designed a series of linear trpzip-like β-hairpin antimicrobial peptides by positioning paired Trp residues at non-hydrogen-bonded sites and Lys residues at hydrogen-bonded sites (Fig. 1) according to the sequence template $(WK)_n^DPG(KW)_n\text{-}NH_2$ ($n = 1, 2, 3, 4, 5$). The Trp and Lys residues were located at every other position in the strands, resulting in all hydrophobic residues falling on the same face in the folded hairpin, while positively charged residues were located on the opposite face, forming an amphipathic structure. The two strands were connected by a rigid ^{D}Pro-Gly turn sequence that stabilizes the type II β-turn and promotes the formation of β-hairpin conformations (Dong et al. 2012; Hilario et al. 2003). Finally, the peptides were amidated at the C-terminal to improve peptide stabilization and increase net positive charge for enhanced antimicrobial activities (Nguyen et al. 2010).

The key physicochemical parameters of the designed peptides are summarized in Table 1. MALDI-TOF MS analysis showed that the measured molecular weights of the synthetic peptides were in close agreement with their theoretical values (Table 1), suggesting that the products correspond to the designed compositions. The hydrophobicity of the peptides in aqueous solution could generally be reflected by the different HPLC retention times. The HPLC retention times for WK1, WK2, WK3, WK4, and WK5 were 10.47, 5.48, 8.00, 9.82, and 10.25 min, respectively, indicating that with the exception of WK1, the hydrophobicity of the synthetic peptides increased with increasing peptide chain length.

Peptide secondary structure in different environments

The secondary structures of the peptides in 10 mM PBS (mimicking the aqueous environment) and 30 mM SDS micelles (mimicking the microbial membrane environment) were investigated by CD spectroscopy. As shown in Fig. 2,

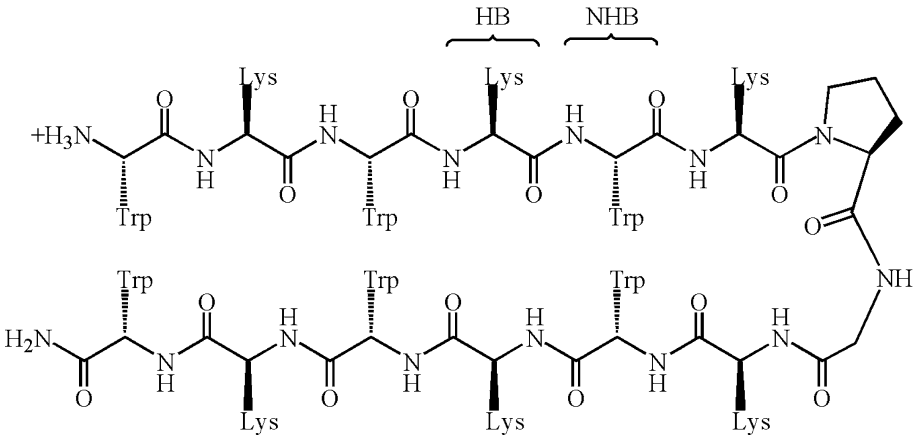

Fig. 1 Sequence and schematic structure of WK3. CD study shows that this peptide exists primarily as a β-hairpin in aqueous buffer. *HB* hydrogen-bonded site, *NHB* non-hydrogen-bonded site

Table 1 Amino acid sequence, molecular weight, HPLC retention time, and net charge of the designed peptides

Peptides	Sequence	Molecular mass (Da)		Retention time (min)	Net charge
		Calculated	Observed		
WK1	$WK^DPGKW\text{-}NH2$	799.96	799.96	10.47	+3
WK2	$(WK)_2^DPG(KW)_2\text{-}NH2$	1428.73	1428.76	5.48	+5
WK3	$(WK)_3^DPG(KW)_3\text{-}NH2$	2057.51	2057.54	8.00	+7
WK4	$(WK)_4^DPG(KW)_4\text{-}NH2$	2686.28	2686.32	9.82	+9
WK5	$(WK)_5^DPG(KW)_5\text{-}NH2$	3315.06	3315.11	10.25	+11

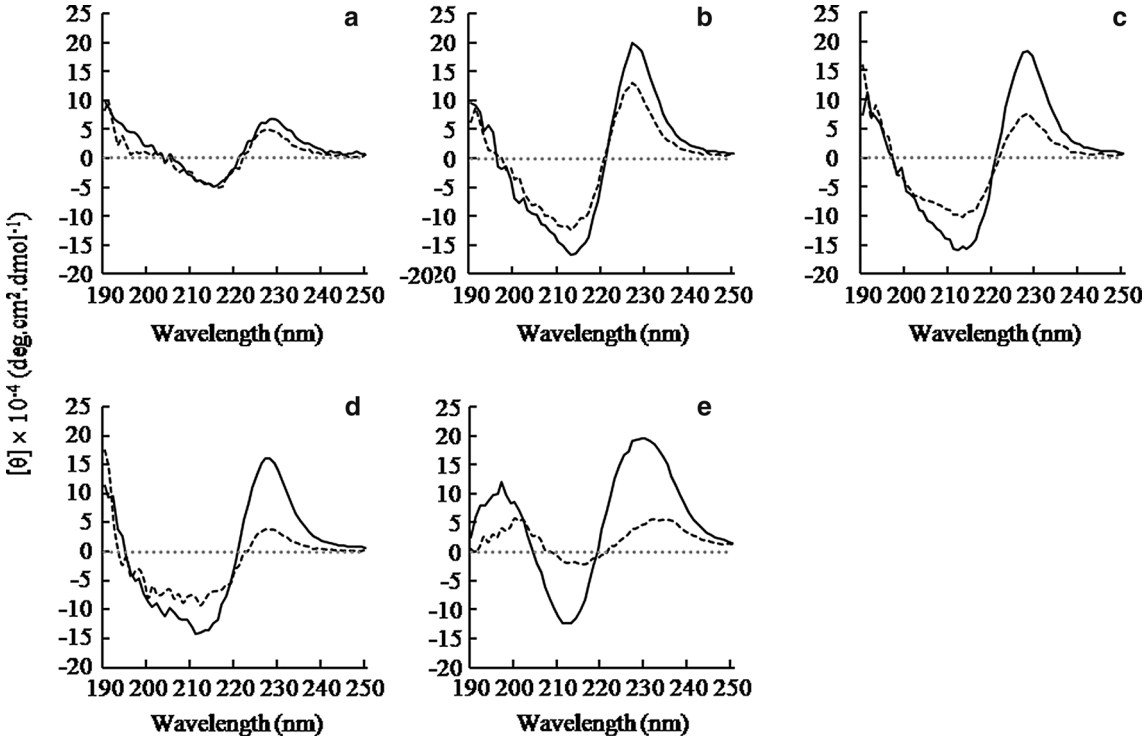

Fig. 2 CD spectra of WK1 (**a**), WK2 (**b**), WK3 (**c**), WK4 (**d**), and WK5 (**e**). The peptides were dissolved in 10 mM PBS (pH 7.4) (*solid line*) and 30 mM SDS (*dotted line*), respectively. The mean residue ellipticity was plotted against wavelength. The values from three scans were averaged per sample

in PBS, the CD spectra of the designed peptides closely match the CD curves of those fully folded tryptophan zippers in shape and are indicative of well-formed β-hairpin structures (Cochran et al. 2001; Dong et al. 2006; Takekiyo et al. 2009). The minimum at ~214 nm is consistent with β-sheet structure (Riemen and Waters 2009), and the characteristic maximum at ~228 nm due to the π–π* exciton coupling originating from the interacting Trp residues is indicative of a distinctive cross-strand Trp–Trp interaction (Wu et al. 2009). In the presence of 30 mM SDS, the main spectral features of the peptides do not exhibit any major changes, suggesting that the native conformations are preserved when the molecules interact with lipid bilayers. The β-sheet percentages were calculated using the second structure predictor server K2D2 (Louis-Jeune et al. 2012). All investigated peptides contained similar β-sheet contents (>43 %) in PBS, whereas the β-sheet content of the longest peptide WK5 (<29 %) was obviously lower than those of the other engineered peptides (>43 %) in SDS.

Antimicrobial and hemolytic activities

The antimicrobial activities of the synthetic peptides against gram-negative and gram-positive bacteria were investigated in terms of their MICs (Table 2). With the exception of WK1, all of the peptides exhibited broad-spectrum antimicrobial activities against the panel of bacteria tested with MICs ranging from 1 to 128 μM. In general, the antibacterial potency of the peptides gradually increased with increasing repeat units up to WK4. However, further increasing the chain length resulted in a significant decrease or even loss of antimicrobial activity, as demonstrated by WK5, which displayed two- to 32-fold higher MIC across the bacterial species compared to WK3 and WK4. The 18-residue peptide WK4 exhibited the strongest antibacterial activity, and the geometric mean of the MIC (GM) value of WK4 was about three times lower than that of PG-1.

The hemolytic activities of the synthetic peptides against hRBCs were measured to provide an indication of their toxicities to mammalian cells (Table 2). The WK1, WK2, and WK3 peptides had no hemolytic activity, even at the highest concentration of 256 μM. In contrast, the longer peptides WK4 and WK5 demonstrated increased hemolytic rates in a dose-dependent manner with MHC (the concentration that induces 5 % or more hemolysis) at 8 and 4 μM, respectively, indicating that the hemolytic activity of the peptides increased with chain length.

We further evaluated the therapeutic index (TI, defined as the ratio of the MHC to the GM) of each peptide to

Table 2 MIC, MHC, and TI of the peptides against gram-negative and gram-positive bacterial strains

Peptides	MIC[a] (μM)						GM[b] (μM)	MHC[c] (μM)	TI[d]
	Gram-negative			Gram-positive					
	E. coli 25922	*E. coli* 1005	*S. Pullorum* 7913	*S. aureus* 29213	*S. aureus* 43300	*S. epidermidis* 12228			
WK1	>128	>128	>128	>128	>128	>128	256	512	2
WK2	2	8	128	32	16	32	18	512	28.51
WK3	1	2	4	4	4	4	2.83	512	181.02
WK4	1	4	4	4	2	2	2.52	8	3.17
WK5	4	8	128	32	8	64	20.16	4	0.2
PG-1	2	4	8	8	8	16	6.345	4	1.59

[a] Minimum inhibitory concentrations (MICs) were determined as the lowest concentration of the peptides that inhibited bacterial growth

[b] The geometric mean (GM) of the peptide MICs against all of the tested bacterial strains was calculated. When no antimicrobial activity was observed at 128 μM, a value of 256 μM was used to calculate the therapeutic index

[c] MHC is the minimum hemolytic concentration that caused 5 % hemolysis of human red blood cells (hRBCs). When no detectable hemolytic activity was observed at 256 μM, a value of 512 μM was used to calculate the therapeutic index

[d] Therapeutic index (TI) is the ratio of the MHC to the GM. Larger values indicate greater cell selectivity

compare the efficacies and safety among different peptide sequences. Among the tested peptides, WK3 had the highest TI of 181.02, which was about 114-fold higher than that of PG-1. WK2 and WK4 displayed moderate TIs of 28.51 and 3.17, respectively. These results showed that WK3 had greater cell selectivity toward bacterial cells over human erythrocyte due to its potent antimicrobial activity and minimal hemolytic activity, implying a wider therapeutic window.

Cytotoxicity

The cytotoxic activities of the peptides on RAW264.7 macrophage cells were assessed by the colorimetric MTT viability assay (Fig. 3). A dose-dependent decrease in cell survival rates was observed for all peptides, and longer peptides (WK4 and WK5) displayed significantly higher cytotoxic activities on RAW264.7 macrophage cells compared to the shorter peptides. At the highest concentration of 128 μM, the cell survival rates of WK1, WK2, and WK3 exceeded 80 %; WK4 and WK5 exhibited greater cytotoxic activities, with cell viabilities of 64.42 and 0.16 %, respectively.

SEM

Based on the MIC and TI values of the peptides, WK4 has the strongest antimicrobial activity, and WK3 has the greatest cell selectivity. Therefore, these two peptides were chosen for further study of their action mechanisms. FE-SEM was performed to directly visualize cell morphology and membrane integrity of *S. aureus* and *E. coli* following

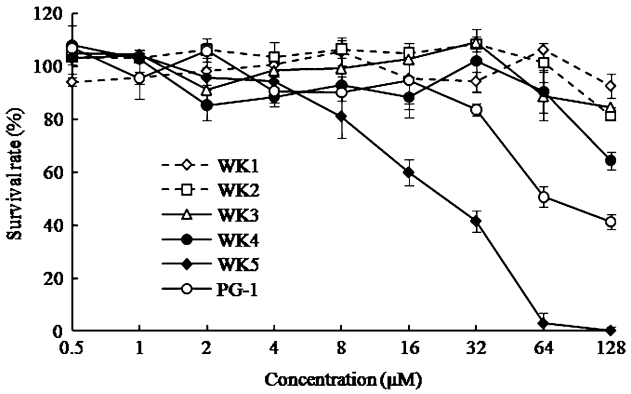

Fig. 3 Cytotoxicity of the peptides against RAW264.7 cells

treatment with peptides at 1 × MICs for 30 min. As shown in Fig. 4, the controls without peptides showed a smooth and intact surface (Fig. 4a, d); in contrast, the peptide treatments induced significant membrane damage. The cytoplasmic membrane surfaces of peptide-exposed *S. aureus* cells appeared roughened, deformed, and covered by numerous blebs (Fig. 4b, c). In addition, well-defined cell membrane breakage was also observed (Fig. 4b), although occurring rarely. The effects of the tested peptides on *E. coli* are shown in Fig. 4e, f. Again, obvious morphological alterations of the treated cells were visualized in the images. Treatment with either peptides induced significant distortion and surface blebbing. Moreover, the plasma membranes appeared to be disintegrated, and fibrous intracellular contents were dispersed outside the cells as a result of cell lysis.

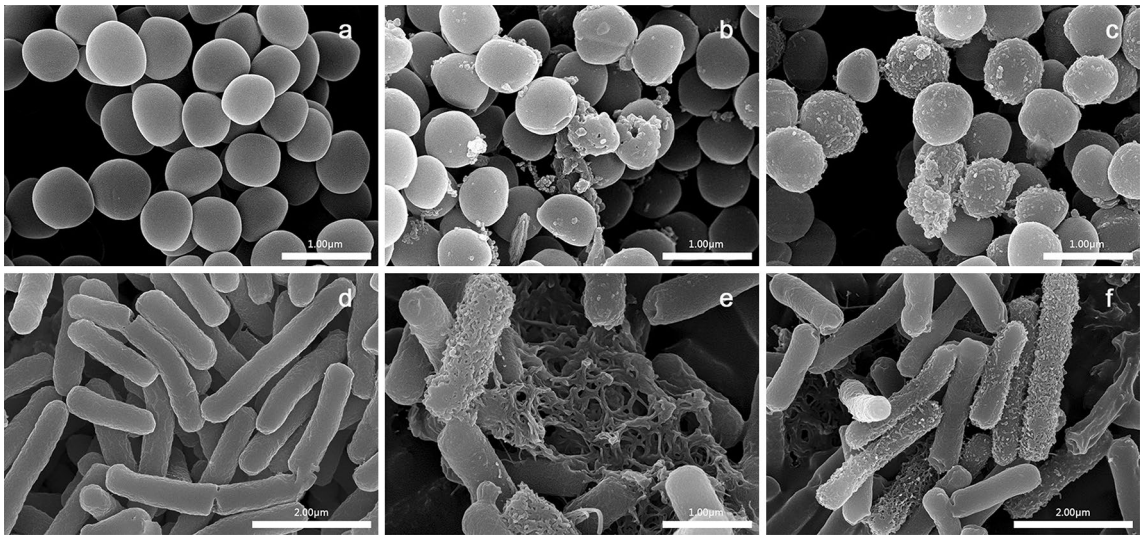

Fig. 4 SEM micrographs of *S. aureus* 29213: **a** control; **b** WK3 treated; **c** WK4 treated. SEM micrographs of *E. coli* 25922: **d** control; **e** WK3 treated; **f** WK4 treated. Bacteria were treated with peptides at 1 × MICs for 30 min. The control was processed without peptides

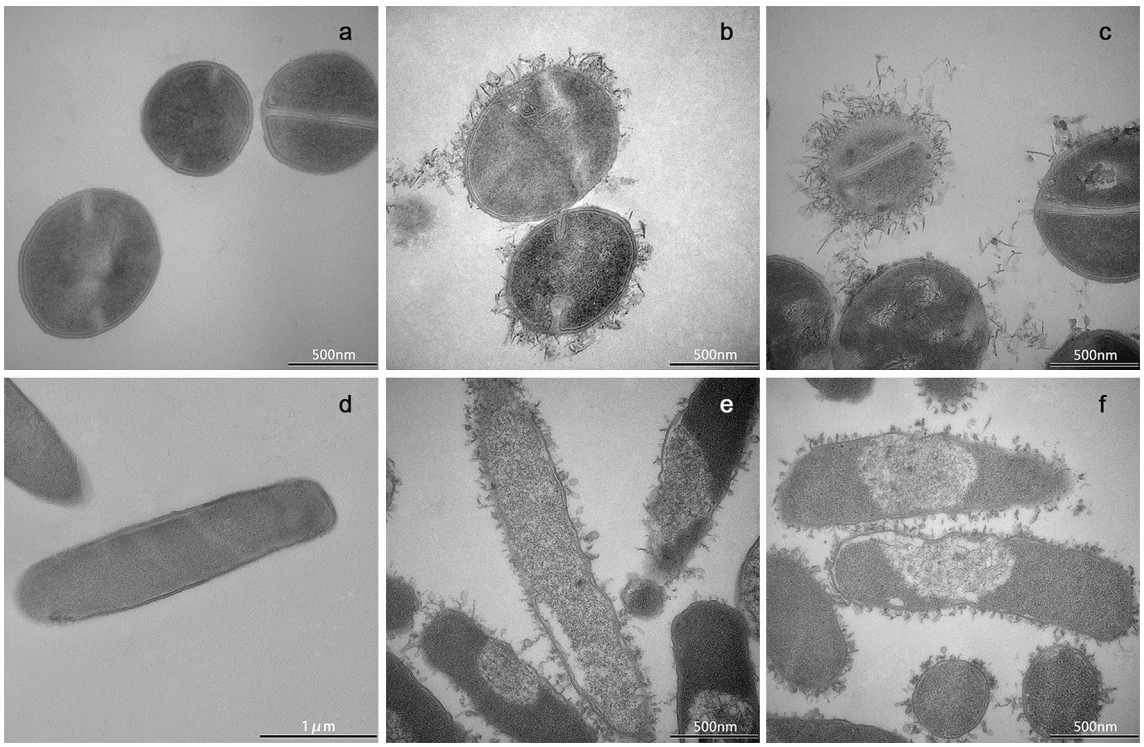

Fig. 5 TEM micrographs of *S. aureus* 29213: **a** control; **b** WK3 treated; **c** WK4 treated. TEM micrographs of *E. coli* 25922: **d** control; **e** WK3 treated; **f** WK4 treated. Bacteria were treated with peptides at 1 × MICs for 30 min. The control was processed without peptides

TEM

The morphological and intracellular alterations of bacterial cells treated with WK3 and WK4 at 1 × MICs were also visualized by TEM. As shown in Fig. 5, intact membrane envelopes and dense internal structures were observed in the untreated bacterial cells (Fig. 5a, d). After 30 min of treatment, the significant collapse of cell membranes and the leakage of intracellular contents were observed in the peptide-treated *S. aureus* cells (Fig. 5b, c). The

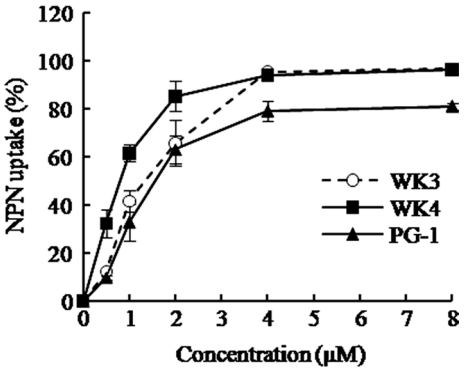

Fig. 6 The outer membrane permeability of WK3, WK4, and PG-1. The uptake of NPN of *E. coli* 1005 in the presence of different concentrations of the peptides was measured using the fluorescent dye (NPN) assay. The NPN uptake was monitored at an excitation wavelength of 350 nm and an emission wavelength of 420 nm

micrographs of peptide-treated *E. coli* indicate that the cytoplasmic membranes were disrupted more severely; the cells appeared empty and deformed due to the leakage of internal contents (Fig. 5e, f).

Permeabilization of outer membranes

NPN uptake assay was performed to evaluate the outer membrane (OM) permeabilization ability of WK3 and WK4. Outer membrane plays a crucial role as a protective barrier in gram-negative bacteria. The fluorescent dye NPN is normally excluded from *E. coli* cells, but exhibits increased fluorescence intensity when it traverses the destabilized outer membrane. The results showed that all of the investigated peptides induced a rapid permeabilizing effect on the outer membrane of *E. coli* in a dose-dependent manner (Fig. 6). In the presence of 2 μM peptide, the outer membrane permeabilities of WK3 and WK4 were more than 70 %. At peptide concentrations above 4 μM, the outer membrane permeabilities of WK3 and WK4 were over 90 %. Compared with PG-1, the designed peptides WK3 and WK4 more effectively permeabilize the outer membrane at the same molar concentrations.

Cytoplasmic membrane electrical potential

The abilities of the peptides to depolarize the bacterial cytoplasmic membrane were determined using the membrane potential-dependent probe $diSC_3$-5, which is quenched in the cytoplasmic membrane. The cytoplasmic membrane potential dissipated when the disruption and permeabilization of the membrane occurred, and $DiSC_3$-5 was then released into the medium, resulting in a conspicuous increase in fluorescence. As shown in Fig. 7, the depolarization of the cytoplasmic membrane of *E. coli* cells by

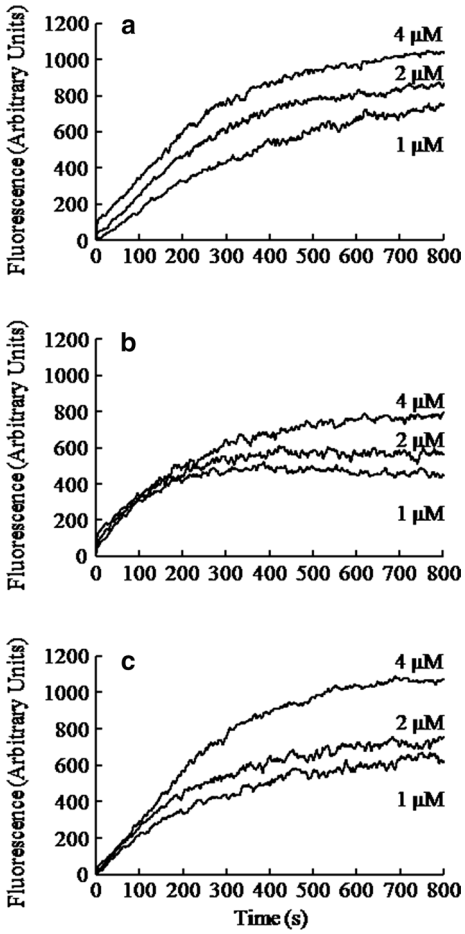

Fig. 7 The cytoplasmic membrane depolarization of *E. coli* 1005 by WK3 (**a**), WK4 (**b**), and PG-1 (**c**). The cytoplasmic membrane potential variation was measured using the membrane potential-sensitive dye diSC3-5. Dye release was monitored at an excitation wavelength of 622 nm and an emission wavelength of 670 nm as a function of time

the peptides was dose- and time-dependent. The peptides WK3 and PG-1 induced rapid increases of similar extents in the fluorescence intensity at all concentrations. In contrast, WK4 induced a slightly smaller increase in fluorescence intensity compared to WK3 and PG-1, which correlated with their antibacterial activities against the same bacteria.

Flow cytometry

The DNA intercalating PI was used to determine the integrity of the bacterial cell membranes. PI stained the nucleic acids in cells when the membrane suffered disruption, causing a conspicuous increase in fluorescence. As shown in Fig. 8, in the absence of peptide, only 1.6 % of the bacterial cells were stained with PI. After treatment with 0.5 × MIC WK3 and WK4, 70.9 and 76.1 % of cells

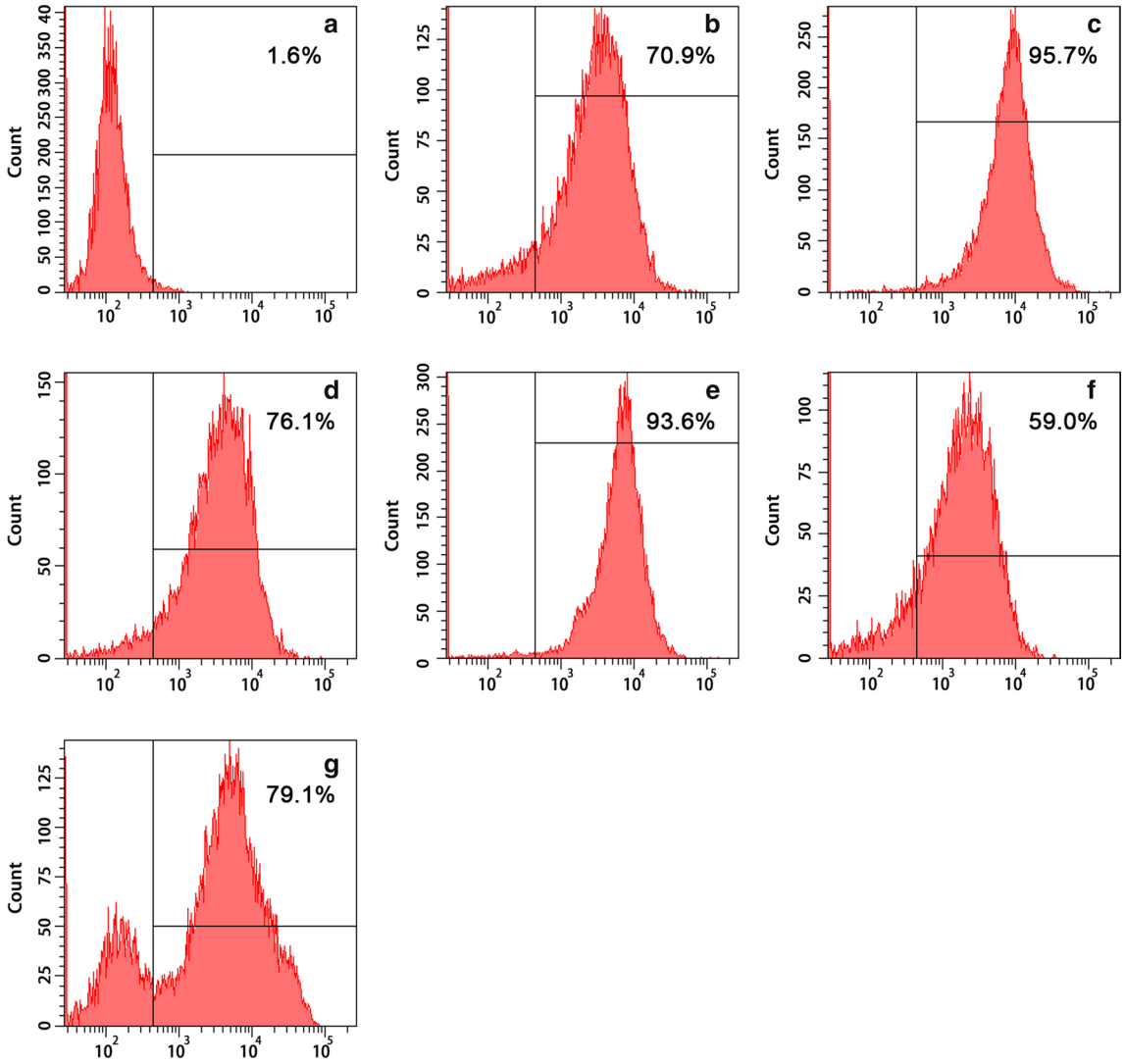

Fig. 8 Flow cytometric analysis. The membrane damage of *E. coli* 25922 treated by peptides was measured by an increase of fluorescent intensity of propidium iodide (PI) at 4 °C for 30 min. **a** No peptide, negative control; **b** WK3 at 0.5 × MIC; **c** WK3 at 1 × MIC; **d** WK4 at 0.5 × MIC; **e** WK4 at 1 × MIC; **f** PG-1 at 0.5 × MIC; **g** PG-1 at 1 × MIC

presented PI fluorescent signals, respectively. More cells (95.7 and 93.6 %) were labeled fluorescently after treatment with WK3 and WK4 when the peptide concentration was increased to 1 × MIC. Both peptides possessed the ability to disrupt the cell membrane of *E. coli* in a dose-dependent manner.

Discussion

Recently, the pairwise Trp–Trp interaction has emerged as a successful strategy for stabilizing the β-hairpin conformation in short peptides. This may be an effective approach for obtaining highly stable bioactive peptides by incorporating the tryptophan zipper motif as a stabilizing structural element. However, it remains unclear whether this method could be used to design β-hairpin antimicrobial peptides and achieve potent antimicrobial activity. In this study, we synthesized a new class of amphipathic linear β-hairpin peptides based on the advantageous features of naturally occurring AMPs and trpzip peptides, as described above, with the aim of investigating the potency of trpzip β-hairpin peptides against pathogenic bacteria and the relationship between peptide length and biological activity.

In the trpzip hairpins, exciton coupling between the pairwise tryptophan indoles results in an intense far UV CD signals at ∼214 and ∼228 nm, indicating a distinctive cross-strand Trp–Trp interaction, which is effectively a tertiary structure; thus, folding can be readily monitored by changes in CD signal (Cochran et al. 2001; Santiveri

and Jiménez 2010). Our data showed that all peptides formed well-defined β-hairpin structures in both water and the membrane-like SDS solution, demonstrating that the designed trpzip peptides are highly stable and that the folding is independent of the induction of anisotropic environments. These results clearly indicated that the pairwise Trp–Trp interactions were sufficient to drive spontaneous folding; thus, the rigid trpzip scaffold can be taken as an ideal template for the design of stable β-hairpin AMPs. Nevertheless, it is worth noting that in SDS, the band of the longest peptide WK5 was shifted to a slightly longer wavelength, and the exciton CD signal was much weaker (only approximately 30 % of the peak intensity) than that in PBS; this indicated that the hairpin conformation was distorted due to loss of stability in the cross-strand interaction (Wu et al. 2012). The calculated β-sheet percentages further confirmed that WK5 has a lower propensity to form the amphipathic β-hairpin structure when the solution environment changes from PBS to SDS. We interpret these data to indicate that the β-hairpin structural stability and propensity of the peptide in bacterial membrane-mimetic environments may play an important role in killing bacterial cells.

The lengths of AMPs play an important role in their costs of production and biological activities. Therefore, considerable studies have been devoted for investigating the quantitative relationship between peptide chain length and antimicrobial activity; nevertheless, such studies are in poor agreement (Gopal et al. 2013; Ma et al. 2013). Several reports have indicated that peptide length is positively correlated with antibacterial and hemolytic activities (Liu et al. 2007; Wiradharma et al. 2011). However, in another study of H-$(LARL)_3$-$(LARL)_n$ series, hemolytic activity increased, while antimicrobial activity decreased with increasing peptide chain length (Niidome et al. 2005). Other work in our lab has shown that the 24-residue-truncated derivative of PMAP-36 displays antimicrobial activity comparable to the parental peptide; however, further truncation of the peptide significantly decreases its antimicrobial activity (Lv et al. 2014). Based on these lines of evidence, the relationship between peptide length and antimicrobial potency is not linear, and there seems to be a threshold effect. As observed in this study, the antibacterial activity of the trpzip peptides initially increased and then decreased with increasing strand length, which was in agreement with our previous studies on β-sheet peptides (Dong et al. 2012). The observed increase in antimicrobial activity with chain length may be attributable to increases in the hydrophobicity and cationicity (Table 1), which are features required for killing bacteria. As indicated by previous reports, an increase in positive charge is beneficial for the initial electrostatic attraction of peptides to the negatively charged membranes of microorganisms (Jiang et al. 2011). In addition, within a certain range, the increasing hydrophobicity of an antibacterial peptide facilitates its insertion into the membrane lipid bilayer, thus imposing antibacterial properties (Chen et al. 2007). In the present study, WK5 has greater hydrophobicity and net cationic charge; thus, we would expect enhanced antimicrobial activity for WK5. However, this was not observed; instead, the antimicrobial activity of WK5 was much weaker than those of the shorter peptides. It is likely that in our case, amphipathicity and structural stability may be important factors in the design of β-hairpin peptides. Numerous studies have persuasively demonstrated that amphipathicity is a prerequisite for AMPs to exert their bactericidal effects, while the overwhelming majority of AMPs become amphipathic only by adopting an appropriate secondary structure (Zelezetsky and Tossi 2006; Jin et al. 2005). Given the CD results, it is clear that WK5 presents a distorted β-hairpin forming character in membrane-mimetic environment, and the propensity for hairpin formation was much lower than those of other peptides, which is in agreement with its capability to inhibit the growth of bacteria. It has been demonstrated that the propensity to form an amphipathic structure in the membrane environment plays a crucial role in the formation of membrane-disruptive activity in AMPs (Takahashi et al. 2010). In addition, distortion of the β-hairpin structure possibly affected the spatial positioning of polar and hydrophobic residues, which led to a disruption of the amphipathic character, thereby compromising the potency and spectrum of activity (Ong et al. 2014). These results suggested that the strand length and structural stability of these β-hairpin peptides are important in determining the level of antimicrobial activity.

Hemolysis and cytotoxicity are usually suggested to be the major parameters of peptide toxicity to eukaryotic cells. In this study, as the number of repeat units increased, the hemolytic activity increased obviously, suggesting that increasing the β-strand length results in a higher toxicity against hRBCs. Several studies have indicated that peptide hydrophobicity is more correlated with increased hemolytic activity rather than antimicrobial activity (Chou et al. 2008). Our results are consistent with that idea. Hydrophobicity is usually measured by detecting the retention time of peptides on a reverse-phase matrix (Liu et al. 2013). We noticed that the hemolytic activities of these β-hairpin peptides seem to be correlated with their retention times; longer retention times promoted the hemolysis of hRBCs. These results indicated that the β-strand length and hydrophobicity played important roles in determining the level of hemolytic activity. Additionally, the cytotoxicity assay with Trpzip peptides further indicated that both length and hydrophobicity affected their cytotoxicities to mammalian cells. Taken together, the broad spectrum and highly selective antimicrobial activity of the 14-mer β-hairpin peptide WK3 at low micromolar concentrations indicate that this

peptide could be developed as a promising antimicrobial agent for therapeutic applications.

As reported in previous studies, the predominant antimicrobial mechanism of cationic AMPs lies in the rapid permeation and disruption of microbial cell membranes, causing the leakage of cytoplasmic contents and eventual cell death. To elucidate the antimicrobial mechanism of trpzip peptides, SEM and TEM were employed to directly visualize changes in cell morphology and membrane integrity of bacteria. Under electron microscopy, significant membrane disruption and intracellular contents leakage were observed in the peptide-exposed bacterial cells compared to the smooth and intact surfaces of the respective control samples (Figs. 4, 5). This observation is consistent with the membrane lytic mechanism of most natural AMPs reported in the literature, implying that the cell membrane may be the primary target of the designed peptides. Further insights were gained by the outer membrane permeability and cytoplasmic membrane depolarization assays. The outer membrane of gram-negative bacteria forms an effective permeability barrier composed of negatively charged phospholipids such as phosphatidylglycerol (PG), cardiolipin (CL), and phosphatidylserine (PS) (Teixeira et al. 2012). Generally, the cationic AMPs bind to the bacterial membrane through electrostatic interactions, leading to membrane permeabilization and transmembrane pore/ion channel formation concomitant with the collapse of the membrane electrical potential (Fjell et al. 2011; Zhu et al. 2014). Our results indicated that the representative peptides WK3 and WK4 induced a rapid permeabilizing effect on the outer membrane of *E. coli*, even at concentrations lower than their MICs (Fig. 6). This suggests that the peptides possess robust capabilities to destroy the outer membrane in the micromolar range. Furthermore, the membrane depolarization assay results (Fig. 7) revealed that these β-hairpin peptides displayed the capacity to dissipate the transmembrane potential via the destruction of the membrane; this would induce intracellular contents leakage, leading to cell death. Additionally, the membrane integrity data based on FACScan analysis (Fig. 8) further confirmed that the peptides killed bacterial cells by damaging cytoplasmic membrane integrity. This rapid physical disruption of bacterial membranes by the peptides is believed to prevent or reduce the likelihood for drug resistance because it is metabolically 'costlier' for microbes to repair or alter their entire membrane composition.

Conclusions

In this study, we have proposed a novel approach to the design of β-hairpin AMPs based upon the tryptophan zipper motif. A series of amphiphilic trpzip-like AMPs were synthesized, and the biological activities and membrane-peptide interactions of the peptides were evaluated. These peptides are short, linear, and spontaneously fold into β-hairpin structures in both aqueous and membrane-mimetic environments. The peptide length has significant influences on the antimicrobial activity and hemolytic activity, and the 14-residue peptide WK3 exhibited a considerably higher level of cell selectivity with TI of 181.02. At its MIC, WK3 rapidly disrupted the microbial membrane, leading to leakage of the intracellular content and eventual cell death. All of these findings demonstrate that WK3 has the potential to be used as a broad-spectrum antimicrobial agent for treating infectious diseases. The present study also provides an effective strategy for β-hairpin peptide design or optimization, which will be useful for the future development of peptide-based antibiotic candidates.

Acknowledgments We gratefully acknowledge the financial support from the National Natural Research Foundation of China (31272453, 31472104), the National Basic Research Program (Grant No. 2012CB124703), the National Science and Technology Support Program (2013BAD10B03), the China Agriculture Research System(CARS-36), the Program of Ministry of Education of China (20092325110009), and the Key Research Program of Heilongjiang Education Bureau (11551z003).

Conflict of interest The authors declare that no conflict of interest exits in the submission of this manuscript.

Compliance with ethical standards All procedures performed in studies involving human participants were in accordance with the ethical standards of the institutional and national research committee and with the 1964 Helsinki declaration and its later amendments or comparable ethical standards. This article does not contain any studies with animals performed by any of the authors. Informed consent was obtained from all individual participants included in the study.

References

Baek JH, Lee SH (2010) Isolation and molecular cloning of venom peptides from *Orancistrocerus drewseni* (Hymenoptera: Eumenidae). Toxicon 55:711–718

Bell G, Gouyon PH (2003) Arming the enemy: the evolution of resistance to self-proteins. Microbiology 149:1367–1375

Brogden NK, Brogden KA (2011) Will new generations of modified antimicrobial peptides improve their potential as pharmaceuticals? Int J Antimicrob Agents 38:217–225

Butterfield SM, Waters ML (2003) A designed β-hairpin peptide for molecular recognition of ATP in water. J Am Chem Soc 125:9580–9581

Chen Y, Guarnieri MT, Vasil AI, Vasil ML, Mant CT, Hodges RS (2007) Role of peptide hydrophobicity in the mechanism of action of α-helical antimicrobial peptides. Antimicrob Agents Chemother 51:1398–1406

Chen C, Hu J, Zeng P, Pan F, Yaseen M, Xu H, Lu JR (2014) Molecular mechanisms of anticancer action and cell selectivity of short α-helical peptides. Biomaterials 35:1552–1561

Chou HT et al (2008) Design and synthesis of cationic antimicrobial peptides with improved activity and selectivity against *Vibrio* spp. Int J Antimicrob Agents 32:130–138

Cochran AG, Skelton NJ, Starovasnik MA (2001) Tryptophan zippers: stable, monomeric β-hairpins. Proc Natl Acad Sci 98:5578–5583

Dong SL, Löweneck M, Schrader TE, Schreier WJ, Zinth W, Moroder L, Renner C (2006) A photocontrolled β-hairpin peptide. Chem A Eur J 12:1114–1120

Dong N, Ma Q, Shan A, Lv Y, Hu W, Gu Y, Li Y (2012) Strand length-dependent antimicrobial activity and membrane-active mechanism of arginine-and valine-rich β-hairpin-like antimicrobial peptides. Antimicrob Agents Chemother 56:2994–3003

Dong N, Zhu X, Chou S, Shan A, Li W, Jiang J (2014) Antimicrobial potency and selectivity of simplified symmetric-end peptides. Biomaterials 35:8028–8039

Eidenschink L, Kier BL, Huggins KNL, Andersen NH (2009) Very short peptides with stable folds: building on the interrelationship of Trp/Trp, Trp/cation, and Trp/backbone-amide interaction geometries. Proteins Struct Funct Bioinform 75:308–322

Fjell CD, Hiss JA, Hancock REW, Schneider G (2011) Designing antimicrobial peptides: form follows function. Nat Rev Drug Discovery 11:37–51

Gopal R, Seo CH, Song PI, Park Y (2013) Effect of repetitive lysine-tryptophan motifs on the bactericidal activity of antimicrobial peptides. Amino Acids 44:645–660

Hilario J, Kubelka J, Keiderling TA (2003) Optical spectroscopic investigations of model β-sheet hairpins in aqueous solution. J Am Chem Soc 125:7562–7574

Hopping G, Kellock J, Caughey B, Daggett V (2013) Designed trpzip-3 β-hairpin inhibits amyloid formation in two different amyloid systems. ACS Med Chem Lett 4:824–828

Jiang Z, Vasil AI, Gera L, Vasil ML, Hodges RS (2011) Rational design of α-helical antimicrobial peptides to target gram-negative pathogens, *Acinetobacter baumannii* and *Pseudomonas aeruginosa*: utilization of charge, 'specificity determinants', total hydrophobicity, hydrophobe type and location as design parameters to improve the therapeutic ratio. Chem Biol Drug Des 77:225–240

Jin Y, Hammer J, Pate M, Zhang Y, Zhu F, Zmuda E, Blazyk J (2005) Antimicrobial activities and structures of two linear cationic peptide families with various amphipathic β-sheet and α-helical potentials. Antimicrob Agents Chemother 49:4957–4964

Kim S, Kim D, Jung HH, Lee IH, Kim JIL, Suh JY, Jon S (2012) Bio-inspired design and potential biomedical applications of a novel class of high-affinity peptides. Angew Chem Int Ed 51:1890–1894

Liu Z, Brady A, Young A, Rasimick B, Chen K, Zhou C, Kallenbach NR (2007) Length effects in antimicrobial peptides of the (RW) n series. Antimicrob Agents Chemother 51:597–603

Liu Y, Xia X, Xu L, Wang Y (2013) Design of hybrid β-hairpin peptides with enhanced cell specificity and potent anti-inflammatory activity. Biomaterials 34:237–250

Louis-Jeune C, Andrade-Navarro MA, Perez-Iratxeta C (2012) Prediction of protein secondary structure from circular dichroism using theoretically derived spectra. Proteins Struct Funct Bioinform 80:374–381

Lv Y, Wang J, Gao H, Wang Z, Dong N, Ma Q, Shan A (2014) Antimicrobial properties and membrane-active mechanism of a potential α-helical antimicrobial derived from cathelicidin PMAP-36. PLoS One 9:e86364

Ma QQ et al (2012) Biochemical property and membrane-peptide interactions of de novo antimicrobial peptides designed by helix-forming units. Amino Acids 43:2527–2536

Ma QQ, Lv YF, Gu Y, Dong N, Li DS, Shan AS (2013) Rational design of cationic antimicrobial peptides by the tandem of leucine-rich repeat. Amino Acids 44:1215–1224

Mirassou Y, Santiveri CM, Pérez de Vega MJ, González-Muñiz R, Jiménez M (2009) Disulfide Bonds versus Trp… Trp pairs in irregular β-hairpins: NMR structure of vammin loop 3-derived peptides as a case study. Chembiochem 10:902–910

Nanda V et al (2005) De novo design of a redox-active minimal rubredoxin mimic. J Am Chem Soc 127:5804–5805

Nguyen LT, Chau JK, Perry NA, De Boer L, Zaat SAJ, Vogel HJ (2010) Serum stabilities of short tryptophan-and arginine-rich antimicrobial peptide analogs. PLoS One 5:e12684

Niidome T, Matsuyama N, Kunihara M, Hatakeyama T, Aoyagi H (2005) Effect of chain length of cationic model peptides on antibacterial activity. Bull Chem Soc Japan 78:473–476

Obrecht D, Chevalier E, Moehle K, Robinson JA (2012) β-Hairpin protein epitope mimetic technology in drug discovery. Drug Discov Today Technol 9:e63–e69

Ong ZY, Gao SJ, Yang YY (2013) Short synthetic β-sheet forming peptide amphiphiles as broad spectrum antimicrobials with antibiofilm and endotoxin neutralizing capabilities. Adv Funct Mater 23:3682–3692

Ong ZY, Cheng J, Huang Y, Xu K, Ji Z, Fan W, Yang YY (2014) Effect of stereochemistry, chain length and sequence pattern on antimicrobial properties of short synthetic β-sheet forming peptide amphiphiles. Biomaterials 35:1315–1325

Riemen AJ, Waters ML (2009) Design of highly stabilized β-hairpin peptides through cation-π interactions of lysine and *N*-methyllysine with an aromatic pocket. Biochemistry 48:1525–1531

Santiveri CM, Jiménez M (2010) Tryptophan residues: scarce in proteins but strong stabilizers of β-hairpin peptides. Pept Sci 94:779–790

Santiveri CM, Leon E, Rico M, Jiménez M (2008) Context-dependence of the contribution of disulfide bonds to β-hairpin stability. Chemistry A Eur J 14:488–499

Santiveri CM, de Vega MJP, González-Muñiz R, Jiménez MA (2011) Trp-Trp pairs as β-hairpin stabilisers: hydrogen-bonded versus non-hydrogen-bonded sites. Org Biomol Chem 9:5487–5492

Takahashi D, Shukla SK, Prakash O, Zhang G (2010) Structural determinants of host defense peptides for antimicrobial activity and target cell selectivity. Biochimie 92:1236–1241

Takekiyo T, Wu L, Yoshimura Y, Shimizu A, Keiderling TA (2009) Relationship between hydrophobic interactions and secondary structure stability for trpzip β-hairpin peptides. Biochemistry 48:1543–1552

Takiguchi T, Morizane S, Yamamoto T, Kajita A, Ikeda K, Iwatsuki K (2014) Cathelicidin antimicrobial peptide LL-37 augments IFN-β expression and anti-viral activity induced by double-stranded RNA in keratinocytes. Br J Dermatol 171:492–498

Teixeira V, Feio MJ, Bastos M (2012) Role of lipids in the interaction of antimicrobial peptides with membranes. Prog Lipid Res 51:149–177

Torrent M, Pulido D, Rivas L, Andreu D (2012) Antimicrobial peptide action on parasites. Curr Drug Targets 13:1138–1147

Wiradharma N, Khoe U, Hauser CAE, Seow SV, Zhang S, Yang YY (2011) Synthetic cationic amphiphilic α-helical peptides as antimicrobial agents. Biomaterials 32:2204–2212

Wu L, McElheny D, Huang R, Keiderling TA (2009) Role of tryptophan-tryptophan interactions in trpzip β-hairpin formation, structure, and stability. Biochemistry 48:10362–10371

Wu L, McElheny D, Setnicka V, Hilario J, Keiderling TA (2012) Role of different β-turns in β-hairpin conformation and stability studied by optical spectroscopy. Proteins Struct Funct Bioinform 80:44–60

Zelezetsky I, Tossi A (2006) Alpha-helical antimicrobial peptides-using a sequence template to guide structure-activity relationship studies. Biochim Biophys Acta 1758:1436–1449

Zhu X, Dong N, Wang Z, Ma Z, Zhang L, Ma Q, Shan A (2014) Design of imperfectly amphipathic α-helical antimicrobial peptides with enhanced cell selectivity. Acta Biomater 10:244–257